Available online at www.sciencedirect.com
ScienceDirect
Journal of Nuclear Materials 363–365 (2007) 1195–1200
journal of nuclear materials
www.elsevier.com/locate/jnucmat

Irradiation effects of low energy helium ions on optical reflectivity of metallic mirror

A. Ebihara [a], M. Tokitani [a], K. Tokunaga [b,*], T. Fujiwara [b], A. Sagara [c], N. Yoshida [b]

[a] Interdisciplinary Graduate School of Engineering Sciences, Kyushu University, Kasuga-koen, Kasuga, Fukuoka 816-8580, Japan
[b] Research Institute for Applied Mechanics, Kyushu University, 6-1 Kasuga-koen, Kasuga-shi, Fukuoka 816-8580, Japan
[c] National Institute for Fusion Science, Oroshi, Toki, Gifu 590-5292, Japan

Abstract

Polycrystalline molybdenum specimens kept at room temperature and 873 K has been irradiated by 1.2 keV- and 8 keV-He^+ up to 3×10^{22} He^+/m^2. Optical reflectivity has been measured with a spectrophotometer for the wave length between 190 and 900 nm. Surface morphology and chemical analyses has been examined with a scanning electron microscope, an atomic force electron microscope and X-ray photoelectron spectrometer. Loss of metallic gloss and remarkable reduction of reflectivity (190–900 nm) occurs by the irradiation of only 1×10^{22} He^+/m^2. Reflectivity decreases with increasing ion energy, irradiation temperature and dose of helium ions. At rather low dose, it is reasonable to suppose that the reflectivity reduction may be due to the surface roughening and fine bubble formation. With increasing dose, roughness became smaller, while reflectivity decreased further. The further reduction of the reflectivity at high dose is considered to be due to the porous structure with nano-scale helium bubbles.

PACS: 78.20.−e; 78.20.Ci; 78.68.+m

Keywords: Bubbles and blisters; Helium beam

1. Introduction

The first mirrors for plasma diagnostics in D-T burning fusion device suffer fairly high flux particle load such as hydrogen isotopes and helium, because they will be placed near the first wall [1]. Effects of the hydrogen isotope irradiation have been studied extensively [2–4] but not much for the helium irradiation because density of helium is one order of magnitude lower than hydrogen isotope in burning plasma condition. Our data of the recent studies on helium irradiation effects in metals indicate that radiation damage by low energy helium ions is very strong and much more serious than that of hydrogen isotopes [5,6]. In the present work, effects of low energy helium ions irradiation on the optical reflectivity have been examined and tried to find their causes.

* Corresponding author.
E-mail address: tokunaga@riam.kyushu-u.ac.jp (K. Tokunaga).

0022-3115/$ - see front matter © 2007 Elsevier B.V. All rights reserved.
doi:10.1016/j.jnucmat.2007.01.153

2. Experimental

The material used in the present experiments was electro-polished polycrystalline molybdenum specimens with very smooth surface. Specimen size was $10 \times 10 \times 0.1$ mm. One half of the specimen was covered and half side (10×5 mm) was irradiated with 1.2 and 8 keV helium ions at RT and 873 K up to the fluence of 3×10^{22} He/m^2 using a duoplasma ion gun equipped with a magnet ion selector. The incident angle of helium ions was normal direction for the sample surface. The ion flux (He^+) was about 2.0×10^{18} He/m^2 s. In addition, hydrogen ions(H_2^+) with 8 keV were also irradiated up to 3×10^{22} H/m^2 at RT.

After the irradiation, optical reflectivity was measured with a spectrophotometer for the wave length between 190 and 900 nm. Angle of incident and reflection from normal direction on specimen surface was in 7.5°. Optical constants (refractive index and extinction coefficient) were calculated by Δ, Ψ measured using a spectroscopic ellipsometer, where Δ corresponds to the phase shift and $\tan \Psi$ the amplitude ratio of the reflected components. Surface morphology was observed with a scanning electron microscope (SEM) and an atomic force microscope (AFM). Microstructure of cross section of specimen near surface irradiated by helium ions was observed with a transmission electron microscope (TEM). Surface chemical and its depth profile analysis were also performed using a X-ray photoelectron spectroscope (XPS). Depth profiles of displacement per atom (DPA) and helium deposition rate (helium atom per molybdenum atom) in molybdenum irradiated with helium ions were calculated by the TRIM-code.

3. Results

Fig. 1 shows the reflectivity of the parts irradiated or not by helium ions at RT (a) and 873 K (b). Loss of metallic gloss occurs and the color of the irradiated surface turned to brown. The reflectivity of the part which is not irradiated by helium ions is about 50% and the spectrum has a structure which depends on wavelength. The reflectivity of the part irradiated by helium ions decreases with increasing fluence and temperature. In particular, decrease of the reflectivity of samples irradiated by 1×10^{22} and 3×10^{22} He/m^2 at 873 K is significantly large. The spectra irradiated by 3×10^{21} He/m^2 at RT and 873 K have structure which depends on wavelength, however, the shape of spectra irradiated by 1×10^{22} and 3×10^{22} He/m^2 is flattened structure.

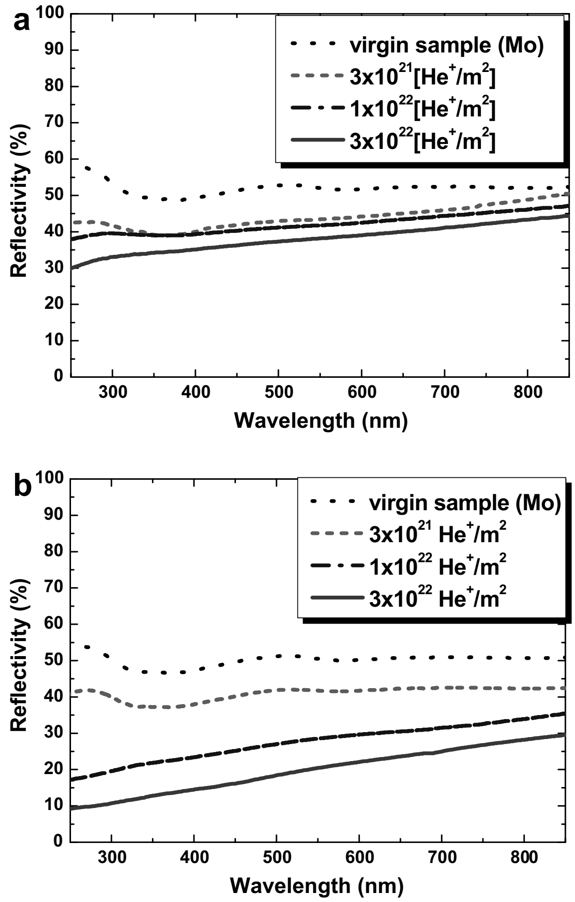

Fig. 1. Reflectivity of the parts irradiated or not by helium ions at RT (a) and 873 K (b).

Shown in Fig. 2 are SEM images of surface morphology before and after the helium ions irradiation. Surface roughening by the formation of blisters occurs by the helium ions irradiation with a fluence of 3×10^{21} He/m^2 and 1×10^{22} He/m^2. Blisters disappears due to sputtering erosion and surfaces become smoother at SEM observation level by the helium ions irradiation with a fluence of 3×10^{22} He/m^2, however, the reflectivity decreased further as described before.

Fig. 3 shows AFM images of the surfaces before and after helium ions irradiation. The rms roughness R is also shown in this figure. The surface is finely modified into the wavy structure as shown in Fig. 3, even if fluence is 3×10^{22} He/m^2 which seems to be smooth by the SEM observation. This

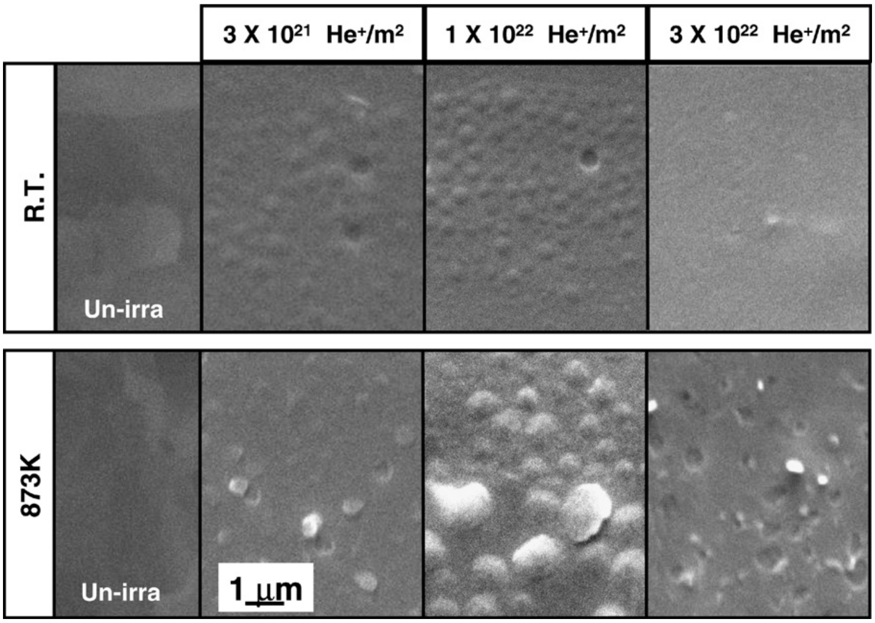

Fig. 2. SEM images of surface morphology before and after the helium ions irradiation.

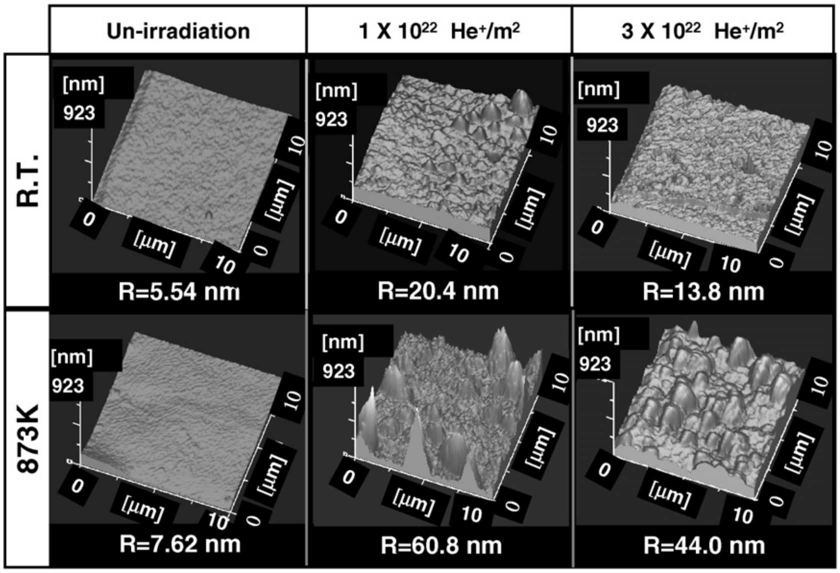

Fig. 3. AFM images of helium ions irradiated surfaces.

is considered to be the result of erosion due to sputtering caused by the helium ions irradiation.

Fig. 4 shows the reflectivity of the parts irradiated by 1.2 keV helium ions and 8 keV H_2^+ ions at RT and 873 K. Reflectivity decreases remarkably even at 1.2 keV He irradiation, however, effect of H_2^+ irradiation is small. Fig. 5 shows the reflectivity of samples irradiated at RT and 873 K at the various wavelengths as a function of the fluence. The reflectivity decreases with the fluence. In particular, decrease at low wavelength area (300 nm) at 873 K is large.

XPS analyses showed that surface after the helium ions irradiation was partially covered by MoO_2 and MoO_3, however, the oxide layer was less than a few nm. The color of the irradiated surface

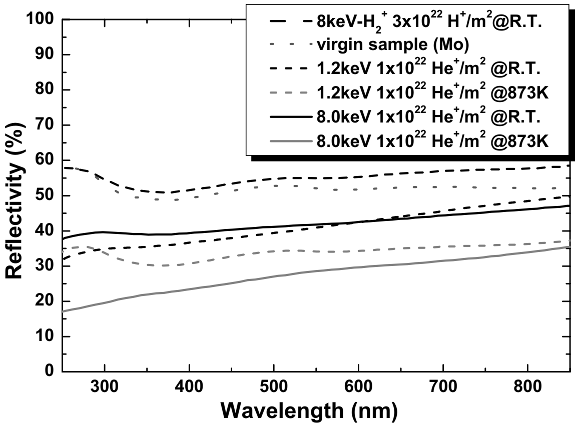

Fig. 4. Reflectivity of the parts irradiated by 1.2 keV helium ions and 8 keV H_2^+ ions at RT and 873 K.

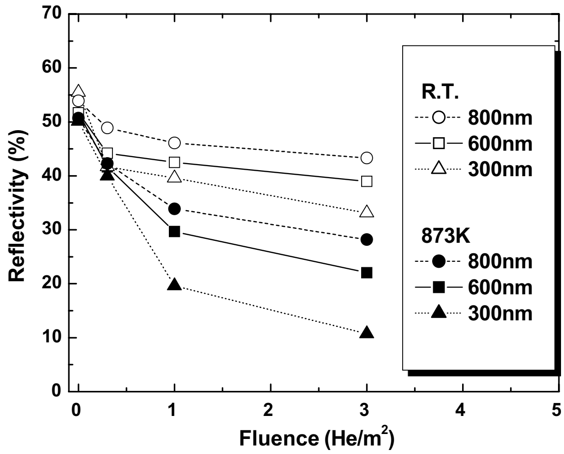

Fig. 5. Reflectivity of samples irradiated at RT and 873 K at the various wavelengths.

do not change even after the elimination of the oxide layer by Ar ions sputtering. This means that change of the color is not the effects of surface contamination and oxidation.

Shown in Fig. 6 is a cross sectional TEM image near the specimen surface irradiated 8 keV helium ions with a fluence of 1×10^{22} He/m^2 at 873 K. Dense bubbles with a diameter of about 2–20 nm are observed in the sub-surface region from the surface up to 200 nm. In addition, swelling also occurred near surface.

Fig. 7 shows optical constants (refractive index (n) and extinction coefficient (k)) of the specimen surface not irradiated (a) or irradiated (b) by 8 keV helium ions with a fluence of 1×10^{22} He/m^2 at 873 K which are calculated by Δ, Ψ measured

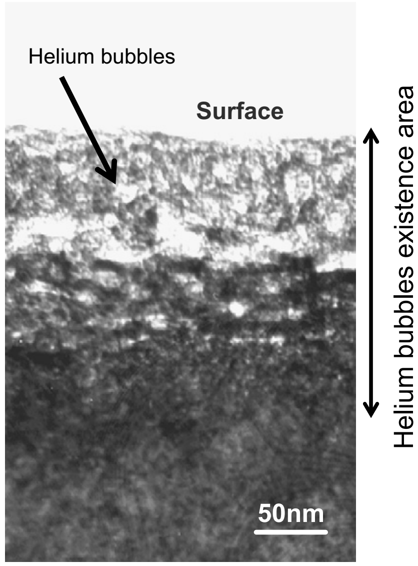

Fig. 6. Cross sectional TEM image near the specimen surface irradiated 8 keV helium ions with a fluence of 1×10^{22} He/m^2 at 873 K.

using the spectroscopic ellipsometer. In the case of the part which was not irradiated, dips of spectrum on extinction coefficient (k) is observed, which indicates the absorption of light by direct interband transitions of within 4d band [7]. In contrast, in the case of the irradiated part, dips of spectrum are not observed. This implies that the distribution of density of states of 4d band changes.

4. Discussion

The depth profiles in molybdenum irradiated 8 keV helium ions calculated by TRIM-code show that helium atoms and primary damage are mostly concentrated near the surface and distributed up to 56 and 54 nm in depth, respectively. Their peaks are at 28 and 14 nm in depth, respectively. On the other hand, the light penetration depth falls to $1/e^2$ of its value can be written $\delta = \lambda/2\pi k$, where λ is the wavelength, k is the extinction coefficient [8]. In the case of Mo [9], δ is 10–40 nm from the surface in the wavelength range from 200 to 900 nm. This sub-surface area influences the reflectivity of molybdenum.

In the case of irradiation of 3×10^{21} He/m^2, formation of fine helium bubbles around the projected range and weak influence on surface roughness occurs. Formation of blisters by the irradiation with a fluence of 1×10^{22} He/m^2 leads large scale rough-

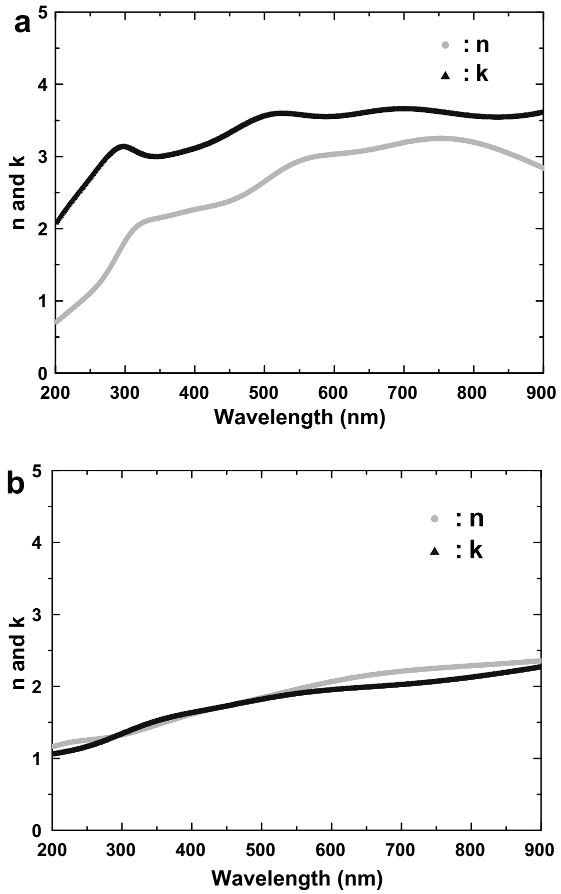

Fig. 7. Optical constants (refractive index (n) and extinction coefficient (k)) of the specimen surface not irradiated (a) or irradiated (b) by 8 keV helium ions with a fluence of 1×10^{22} He/m^2 at 873 K which are calculated by Δ, Ψ measured using a spectroscopic ellipsometer.

ening. The reduction of the reflectivity in the case of irradiation of 3×10^{21} He/m^2 and 1×10^{22} He/m^2 is considered to be due to the diffused reflection by the roughening and the multiple scattering of light by bubbles in the sub-surface region.

Up to a fluence of 3×10^{22} He/m^2, due to the sputtering erosion, the covers of blisters disappear. Due to the balance of formation of bubbles and sputtering erosion, dense fine bubbles always exist in the area between the surface and the projected range. Sub-surface area becomes to be porous structure as shown in Fig. 6. He bubbles beneath the surface cause the fine scale surface roughening as shown in Fig. 3. However, the value of the rms roughness of the sample irradiated with a fluence of 3×10^{22} He/m^2 is smaller than that of the sample irradiated with a fluence of 1×10^{22} He/m^2. Therefore, it seems that the stronger reduction of the reflectivity at higher dose (3×10^{22} He/m^2), where the blisters have almost disappeared, can not be explained only by the surface roughness. In the case of at a high temperature of 873 K, helium and vacancies diffuse to deeper area and bubbles are formed in the sub-surface region from the surface up to 200 nm as shown in Fig. 6. Microstructure such as bubble size and distribution near surface within the light penetration depth at a high temperature of 873 K is also different from that of at a low temperature of RT. Therefore, it is reasonable to suppose that the stronger reduction of the reflectivity at higher dose with a high temperature of 873 K is attributed to the multiple scattering of light by the dense fine bubbles in the sub-surface region.

In comparison with hydrogen irradiation, remarkable degradation of the optical reflectivity by hydrogen ions irradiation with similar energy occurs at the fluence above 10^{25} ions/m^2 [2,10]. We should note that effects of helium are three orders of magnitude higher than that of hydrogen.

The spectroscopic ellipsometry analyses showed that the distribution of density of states of 4d band of the sample, irradiated by helium ion, changed to be flat. In the sub-surface area, crystal structure may be distorted by the formation of dislocation and high pressure bubbles due to the helium ions irradiation. This is one possible mechanism for the change of the distribution of density of states of 4d band.

5. Conclusion

In order to know the effects of helium ion bombardment on the optical reflectivity and the underlining mechanisms, reflectivity, surface morphology, surface chemical analysis and sub-surface damage have been examined for molybdenum. Loss of metallic gloss and remarkable reduction of reflectivity (190–900 nm) occurs by the irradiation of only 1×10^{22} He/m^2. Reflectivity decreases with increasing ion energy, irradiation temperature and dose of helium ions. At rather low dose, it is reasonable to suppose that the reflectivity reduction may be due to the surface roughening and fine bubble formation. With increasing dose, roughness became smaller, while reflectivity decreased further. The further reduction of the reflectivity at high dose is considered to be due to the porous structure with nano-scale helium bubbles. Remarkable degradation of the optical reflectivity by hydrogen ions irradiation with similar energy occurs at the fluence above 10^{25} ions/m^2. We should note that effects of helium are three orders of magnitude higher than that of hydrogen. It is necessary that detail understanding of physical relation between the reflectivity and sub-surface structure will be carried. In addition, phenomena in plasma confinement devices such as synergistic effects of helium bombardment and re-deposition will be investigated. Furthermore, R&D for the method reducing the effects will be also required.

Acknowledgement

The authors gratefully acknowledge the assistance of J.A. WOOLLAM Japan in performing spectroscopic ellipsometry analyses.

References

[1] A.E. Costley, D.J. Campbell, S. Kasai, K.E. Young, V. Zaveriaev, Fusion Eng. Design 55 (2001) 331.
[2] V.S. Voitsenya, A.F. Bardamid, V.T. Gritsyna, V.G. Konovalov, O. Motojima, D.V. Orlinskij, R. Palladino, B.J. Peterson, A.N. Shapoval, A.F. Shtan, S.I. Solodovchenko, K.I. Yakimov, K. Young, J. Nucl. Mater. 258–263 (1998) 1919.
[3] V.S. Voitsenya, A.F. Bardamid, V.N. Bondarenko, W. Jacob, V.G. Konovalov, S. Masuzaki, O. Motojima, D.V. Orlinskij, V.L. Poperenko, I.V. Ryzhkov, A. Sagara, A.F. Shtan, S.I. Solodovchenko, M.V. Vinnichenko, J. Nucl. Mater. 290–293 (2001) 336.
[4] T. Sugie, S. Kasai, M. Taniguchi, M. Nagatsu, T. Nishitani, J. Nucl. Mater. 329–333 (2004) 1481.
[5] K. Tokunaga, S. Tamura, N. Yoshida, K. Ezato, M. Taniguchi, K. Sato, S. Suzuki, M. Akiba, J. Nucl. Mater. 329–333 (2004) 757.
[6] N. Yoshida, H. Iwakiri, K. Tokunaga, T. Baba, J. Nucl. Mater. 337–339 (2005) 946.
[7] F. Wooten, Optical Properties of Solid, Academic Press, 1972.
[8] M. Born, E. Wolf, Principles of Optics, 7th Ed., Cambridge University, 1999.
[9] E.D. Palik (Ed.), Handbook of Optical Constants of Solids, Academic Press, 1985.
[10] A.F. Bardamid, A.I. Belyaeva, V.N. Bondarenko, J.W. Davis, A.A. Galuza, I.E. Garkusha, A.A. Haasz, V.G. Konovalov, A.D. Kudlenko, M. Poon, I.V. Ryzhkov, S.I. Solodovchenko, A.F. Shtan, V.S. Voitsenya, K.I. Yakimov, Phys. Scr. T103 (2003) 109.